Endophilin I mediates synaptic vesicle formation by transfer of arachidonate to lysophosphatidic acid

Anne Schmidt*†, Michael Wolde‡†, Christoph Thiele*, Werner Fest‡, Hartmut Kratzin§, Alexandre V. Podtelejnikov‖¶, Walter Witke‖¶, Wieland B. Huttner* & Hans-Dieter Söling‡

* *Max-Planck-Institute of Molecular Cell Biology and Genetics, Pfotenhauerstrasse 110, D-01307 Dresden, and Department of Neurobiology, University of Heidelberg, Im Neuenheimer Feld 364, D-69120 Heidelberg, Germany*
‡ *Department of Clinical Biochemistry, University of Göttingen, and Max-Planck-Institute of Biophysical Chemistry, Am Fassberg 11, D-37077 Göttingen, Germany*
§ *Max-Planck-Institute for Experimental Medicine, Herman-Rein-Strasse 3, D-37075 Göttingen, Germany*
‖ *European Molecular Biology Laboratory, Meyerhofstrasse 1, D-69012 Heidelberg, Germany*
† *These authors contributed equally to this work.*

Endophilin I is a presynaptic protein of unknown function that binds to dynamin, a GTPase that is implicated in endocytosis and recycling of synaptic vesicles. Here we show that endophilin I is essential for the formation of synaptic-like microvesicles (SLMVs) from the plasma membrane. Endophilin I exhibits lysophosphatidic acid acyl transferase (LPAAT) activity, and endophilin-I-mediated SLMV formation requires the transfer of the unsaturated fatty acid arachidonate to lysophosphatidic acid, converting it to phosphatidic acid. A deletion mutant lacking the SH3 domain through which endophilin I interacts with dynamin still exhibits LPAAT activity but no longer mediates SLMV formation. These results indicate that endophilin I may induce negative membrane curvature by converting an inverted-cone-shaped lipid to a cone-shaped lipid in the cytoplasmic leaflet of the bilayer. We propose that, through this action, endophilin I works with dynamin to mediate synaptic vesicle invagination from the plasma membrane and fission.

Membrane traffic mediated by vesicular carriers is a fundamental process in all eukaryotic cells. Any given trafficking step requires two processes of membrane fusion; that leading to the pinching-off of the vesicle from its donor membrane, called fission, and that resulting in the merging of the vesicle with its acceptor membrane. With regard to membrane fission, two principal models can be distinguished. These are not necessarily mutually exclusive but may reflect basic differences between the various types of intracellular donor membranes and vesicles.

One model views the process of membrane fission as the ultimate consequence of membrane budding. Here, the continuation of the change of shape of the donor membrane by a proteinaceous coat machinery that mediates budding is thought to constrict the lipid bilayer at the edge of the polymerizing coat, that is, the neck of the nascent vesicle, sufficiently for membrane fission to occur. Studies on vesicle formation in the early secretory pathway have provided considerable evidence in support of this model, notably the demonstration that the coat proteins (COP I and COP II) are sufficient to generate small lipid vesicles from liposomes, if the liposomes bear an integral membrane constituent (lipid or membrane-anchored protein motif) that is appropriate for coat recruitment[1–3].

The other model views membrane budding and membrane fission as being separate, though often linked, processes that are mediated by distinct proteinaceous machineries with the potential, but not the need, to interact. Here, following the coat-mediated formation of a membrane bud, membrane fission results from the action of a separate set of proteins that mediate the constriction of the narrow membrane tubule connecting the nascent vesicle with the donor membrane. Evidence supporting this model has largely been obtained in studies on endocytosis, in particular the recycling of synaptic vesicles from the plasma membrane[4–8]. Whereas the clathrin coat mediates bud formation[7,9], a ring around the neck of the nascent vesicle, formed upon polymerization of the GTPase dynamin[10,11], is thought to be central in membrane constriction and fission[4–6,8].

It has been proposed that this membrane constriction and fission is driven by a change in the conformation of dynamin that occurs upon GTP hydrolysis[4,5,8,11–14]. However, the view that dynamin itself acts as a 'pinchase' has been questioned[15]. In fact it appears that dynamin does not function as a force-generating GTPase but rather, like other members of the GTPase superfamily, activates an as yet unknown effector system when in the GTP-state, and it is this effector system that is essential for fission[16,17]. If so, dynamin-interacting proteins, such as the endophilin I (originally called SH3p4, ref. 18) that is studied here, are obvious candidates for this effector system.

The shape of a membrane is influenced not only by proteins but also by lipids. The shape of membrane lipids is a key determinant of membrane curvature[19–21]. Inverted-cone-shaped lipids favour positive curvature, which characterizes the outer leaflet of a membrane bud, and cone-shaped lipids favour negative curvature, as found in the inner leaflet of a bud. Examples of inverted-cone-shaped lipids and cone-shaped lipids include lysophospholipids and unsaturated fatty acids, respectively[20,22]. Indeed, in one of the paradigms of membrane fusion, that of the influenza virus envelope with the plasma membrane mediated by the viral haemagglutinin[23,24], the differentially shaped lipids lysophosphatidylcholine (inverted cone) and oleic acid (cone) affect the fusion process in an opposite (negative and positive, respectively) manner[22]. The shape of these lipids is thought to affect critically the transition between the intermediates in lipid bilayer organization that have been hypothesized to exist during the fusion process[20,21].

This raises two questions. First, do differently shaped lipids also have a role in membrane fission? Second, how is lipid shape controlled? Here we report on the role of endophilin I in the control of lipid shape and changes in membrane curvature underlying the formation of synaptic vesicles from the plasma membrane.

¶ Present address: Protein Interaction Laboratory, University of Southern Denmark, Campusvej 55, Odense, DK-5230 Denmark (A.V.P.); Mouse Biology Programme, European Molecular Biology Laboratory, Via Ramarini 32, I-00016 Monterotondo, Italy (W.W.)

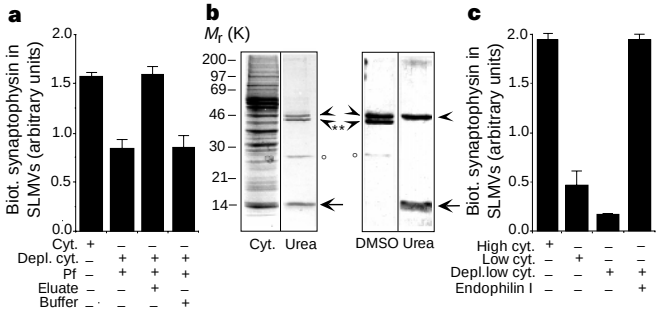

Figure 1 Endophilin I is rate-limiting for SLMV biogenesis. **a**, SLMV formation in perforated PC12 cells using either complete (Cyt.) or poly(L-proline)-depleted (Depl. cyt.) brain cytosol (1.8 mg protein per ml) supplemented as indicated with 3 μg ml^{-1} recombinant profilins (Pf, 30:1 ratio of mouse profilin II to human profilin I), dialysed 30% DMSO eluate from the poly(L-proline) column containing ~8 μg 40K protein per ml (Eluate), and/or the equivalent amount of dialysed 30% DMSO elution buffer (Buffer). **b**, SDS-PAGE followed by Coomassie-Blue staining of complete brain cytosol (Cyt.), the 8 M urea eluate from the poly(L-proline) column (left, Urea), the 30% DMSO eluate from the poly(L-proline) column (DMSO), and the 8 M urea eluate from the poly(L-proline) column obtained after elution with 30% DMSO (right, Urea). Arrowheads, actin; arrowheads with asterisk, 40K protein; circles, 28K protein; arrows, profilins. **c**, SLMV formation in perforated PC12 cells using brain cytosol supplemented with 25 μg ml^{-1} purified (poly(L-proline)) recombinant His_6–endophilin I as indicated: complete high-protein cytosol (High cyt., 3.75 mg protein per ml) or low-protein cytosol (Low cyt., 0.75 mg protein per ml), poly(L-proline)-depleted low-protein cytosol (Depl. low cyt., 0.75 mg protein per ml). In **a** and **c**, data are the mean of two independent perforated-cell reactions; error bars indicate the variation of the individual values from the mean.

Endophilin I is required for SLMV formation

To identify rate-limiting factors for SLMV formation, we used a previously established perforated-cell system, derived from the rat neuroendocrine cell line PC12, which reconstitutes this process[25]. This perforated-cell system is based on cell-surface biotinylation of the synaptic vesicle membrane protein synaptophysin, and its accumulation in a specialized domain of the plasma membrane at 18 °C (ref. 26), followed by its incorporation into SLMVs upon cell perforation, addition of brain cytosol and ATP, and a return of the temperature to 37 °C. In investigating whether the dynamin-interacting[27], actin-binding protein profilin was involved in SLMV formation, we noted that cytosol depleted of profilin by passage over poly(L-proline) Sepharose[28] was much less efficient than control cytosol but that addition of recombinant profilin to the depleted cytosol did not fully restore SLMV formation (Fig. 1a). This indicated that passage of cytosol over poly(L-proline) Sepharose led to the depletion of a protein (or proteins) other than profilin that is required for SLMV formation.

Elution of the proteins bound to poly(L-proline) Sepharose with 8 M urea revealed four major bands with relative molecular masses (M_r) of 45K, 40K, 28K and 15K (Fig. 1b). Immunoblotting (data not shown) revealed the identity of the 45K and the 15K bands as actin and profilin, respectively. Selective elution of the 40K protein and the 28K protein, along with some actin but without profilin, was achieved using 30% dimethyl sulphoxide (DMSO) (Fig. 1b). Addition of the DMSO eluate to depleted cytosol supplemented with recombinant profilin fully restored SLMV formation (Fig. 1a).

High-accuracy matrix-assisted laser desorption/ionization (MALDI) peptide-mass mapping revealed that the 40K protein was endophilin I (originally called SH3p4, refs 8, 18, 29), with 51%, 48% and 44% of the complete human (accession no. Q99962), complete mouse (accession no. Q62420) and partial rat (accession no. AF009603) sequence, respectively, being covered. Similarly, the 28K protein was unambiguously identified as the SH3- and SH2-domain-containing protein Grb2 (data not shown).

Endophilin I interacts with dynamin[30], synaptojanin[30,31] and amphiphysin[29], which have been implicated in synaptic vesicle recycling[6,8,32]. The identification of the 40K protein as endophilin I indicated that this protein might be the relevant component in the DMSO eluate with regard to SLMV formation. We therefore investigated the effect of recombinant endophilin I on SLMV formation in the perforated-cell system using low-protein cytosol (cytosol that is suboptimal for SLMV formation[25]). SLMV formation in the presence of low-protein cytosol that had been completely depleted of endogenous endophilin I by passage over poly(L-proline) Sepharose (as revealed by immunoblotting; data not shown) was almost as low (Fig. 1c) as the background value obtained in the absence of added cytosol. Addition to depleted cytosol of a concentration of recombinant endophilin I corresponding to that in high-protein cytosol increased SLMV formation in the perforated-cell system to that observed with high-protein cytosol[25] (Fig. 1c). This showed not only that endophilin I is the critical cytosolic component depleted by passage over poly(L-proline) Sepharose, but also that this protein is rate-limiting for SLMV formation. Confirming the latter conclusion, addition of increasing amounts of recombinant endophilin I (up to 16 μg ml^{-1}) to low-protein cytosol resulted in a progressive stimulation of SLMV formation, which approached the level obtained with high-protein cytosol (data not shown). SLMV formation was also stimulated by recombinant endophilin I in a modified cell-free system, in a similar manner to the perforated-cell system (data not shown). In this system, PC12 cells were biotinylated at 18 °C and homogenized (rather than only perforated), and the homogenate was subjected to cell-free reaction followed by isolation of SLMVs without further homogenization (analogous to the cell-free system of ref. 33).

Table 1 Purification of LPAAT from bovine brain

Purification step	Protein (mg)	Total LPAAT activity (mU)	Specific LPAAT activity (mU mg^{-1} protein)
Extract	16,520	1,962	0.12
Q-Sepharose (peak II)	5,284	1,532	0.29
S-Sepharose	480	566	1.18
Mono Q HR	129	122	0.95
Superdex 75	8.8	59	6.65
Mono Q HR	5.8	37	6.38
ESPACE	3.3	55	16.51

Endophilin I has LPAAT activity

An independent line of investigation originated from the observations[34–36] that stimulation of exocytosis in parotid acinar cells is associated with an increase in the activity of lysophosphatidic acid acyl transferase (LPAAT), which converts lysophosphatidic acid (LPA) to phosphatidic acid. The increase in LPAAT activity upon stimulation of secretion is due to phosphorylation by cyclic-AMP-dependent protein kinase or Ca^{2+}/calmodulin-dependent protein kinase II (refs 35, 36). To identify this phosphorylation-sensitive LPAAT, we purified it (Table 1). Bovine brain tissue was used as the source because LPAAT activity increases upon addition of either protein kinase to a brain-derived total post-nuclear membrane fraction[36]. Q-Sepharose ion-exchange chromatography gave two peaks of LPAAT activity, one (peak I) of which also contained lysophosphatidylcholine (LPC) acyl transferase activity and was not significantly stimulated by phosphorylation, and the other (peak II) of which did not exhibit significant LPC acyl transferase activity but was stimulated by phosphorylation (data not shown). LPAAT in peak II was purified to apparent homogeneity (Table 1). The final purificaton step consisted of preparative, continuous elution SDS-polyacrylamide gel column electrophoresis (ESPACE). The fractions obtained were examined for protein content by analytical SDS-polyacrylamide gel electrophoresis (PAGE) (Fig. 2a) and for LPAAT activity after protein renaturation (Fig. 2b). This revealed a single ~40K protein band (Fig. 2a), which coincided with LPAAT activity (Fig. 2b), in fractions 18–30. Two-dimensional (2D) PAGE showed that the 40K protein band consisted of a single protein with

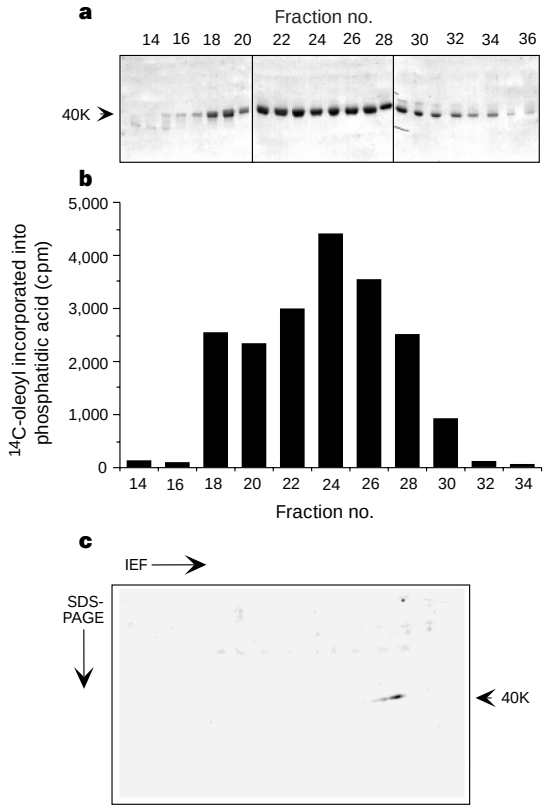

Figure 2 Identification of purified bovine brain LPAAT as endophilin I. **a**, **b**, ESPACE, the final step in the purification. Aliquots of some of the ~150 fractions obtained after ESPACE were subjected to analytical SDS-PAGE on three minigels followed by Coomassie-Blue staining (**a**, entire separating gels are shown), and the remainder of the indicated fractions was renatured and aliquots of equal volume (containing 3.3 μg protein in the case of fraction 24) analysed for LPAAT activity (**b**). **c**, 2D PAGE followed by Coomassie-Blue staining of the pooled fractions containing the peak of LPAAT activity (5 μg protein).

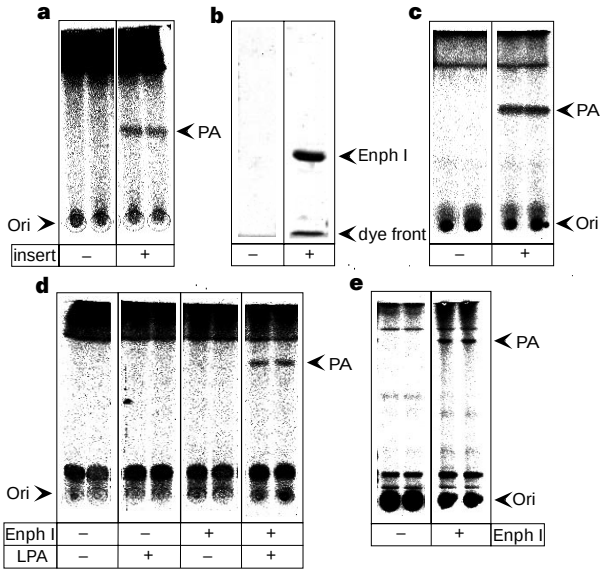

Figure 3 Endophilin I exhibits LPAAT activity. **a**, **c**, Duplicate LPAAT assays using 5 μM [^{14}C]arachidonoyl-CoA, 10 μM LPA and protein from a lysate (freezing/thawing) of bacteria transformed without (insert –) or with (insert +) the insert coding for His$_6$–endophilin I; **a**, 280,000*g* supernatant (~0.5 mg ml^{-1} protein); **c**, 15 μg ml^{-1} purified (poly(L-proline)) recombinant His$_6$–endophilin I. **b**, Coomassie-Blue stained SDS-polyacrylamide gel of the purified recombinant His$_6$-endophilin I (~10 μg protein) used in **c**. **d**, Duplicate LPAAT assays using 5 μM [^{14}C]arachidonoyl-CoA in the absence (–) and presence (+) of 10 μM LPA and 10 μg ml^{-1} recombinant (metal-chelate) His$_6$–endophilin I as indicated. **e**, Duplicate LPAAT assays using 50 μM [^{14}C]arachidonoyl-CoA and 100 μM LPA in the absence (–) and presence (+) of the 30% DMSO eluate (~5 μg endophilin I per ml) obtained from the poly(L-proline) column loaded with brain cytosol. **a**–**e**, Enph I, endophilin I; PA, phosphatidic acid; Ori, origin.

an acidic isoelectric point (Fig. 2c). The sequence of five tryptic peptides obtained from the purified 40K protein (AVMEIMTKT IEYL, IRGQEKGPGYPQAEA, GPGYPQAEALLAEAML, QGKIPD EELRQALE, EIAESSMFNLLEMD) was identical to that of predicted tryptic fragments of endophilin I. This, together with the finding that the reported molecular mass (40K, refs 30, 31) and predicted isoelectric point (pI 5.33) of endophilin I are, within the range of experimental accuracy, identical to those of the 40K band that comigrates with LPAAT activity upon purification, indicates that LPAAT activity is intrinsic to endophilin I.

When oleoyl-CoA was used as a co-substrate, the purified bovine brain enzyme exhibited a high specificity for LPA as substrate as compared to other lysophospholipids (Table 2). Moreover, like the enzyme studies in tissue[34–36] and crude subcellular fractions[35,36], the activity of the purified enzyme was stimulated by phosphorylation with cAMP-dependent protein kinase (Table 2) or Ca^{2+}/calmodulin-dependent protein kinase II (data not shown). Activation of the purified enzyme was accompanied by [^{32}P]phosphate incorporation into the 40K band that approached a value of 1 mol of phosphate per mol of protein (data not shown).

To confirm that endophilin I has LPAAT activity, recombinant endophilin I was expressed in bacteria as either His$_6$-tagged or glutathione *S*-transferase (GST)-fusion protein and analysed for LPAAT activity. To exclude a contribution of endogenous bacterial LPAAT, which is a transmembrane protein[37], the bacteria were lysed by freezing-thawing in the absence of detergent, followed by ultracentrifugation. The high-speed supernatant obtained from bacteria transformed with vector containing the insert encoding His$_6$-tagged endophilin I exhibited LPAAT activity in the presence of LPA and arachidonoyl-CoA as exogenous substrates, whereas that obtained after transformation with vector lacking the insert did not (Fig. 3a). The same results were obtained when oleoyl-CoA was used instead of arachidonoyl-CoA (data not shown).

Recombinant His$_6$-tagged endophilin I was purified from the bacterial high-speed supernatant by affinity chromatography on poly(L-proline) Sepharose (Fig. 3b). Purified recombinant endophilin I exhibited LPAAT-activity (Fig. 3c). In contrast, a poly(L-proline) eluate obtained from the high-speed supernatant of bacteria transformed with vector lacking insert, which did not contain endophilin I (Fig. 3b), did not show detectable LPAAT activity (Fig. 3c). Similar results were obtained with recombinant His$_6$-tagged endophilin I purified by metal chelate affinity chromato-

Table 2 Lysophospholipid specificity of purified and recombinant endophilin I and its activation by phosphorylation

Protein	LPA		LPC	LPS	LPI	LPE
	Control	PKA				
Purified endophilin I	100	306	5.8	7.2	1.0	5.5
His$_6$–endophilin I	100	204	4.2	3.9	0.9	1.5
GST–endophilin I	100	205	3.3	3.3	2.6	3.2

Specific LPAAT activity is expressed as percentage of control, using LPA as substrate. Specific LPAAT activities for the control condition were 4.95, 10.80 and 5.46 for endophilin I purified from bovine brain, His$_6$–endophilin I and GST–endophilin I, respectively, PKA, cyclic AMP-dependent protein kinase.

graphy, and with a GST–endophilin-I fusion protein purified from bacterial high-speed supernatant by affinity chromatography on either GSH-agarose or poly(L-proline) Sepharose (data not shown).

The LPAAT activity of recombinant, His_6-tagged or GST-fused endophilin I, purified by affinity chromatography on metal chelate- or GSH-matrices, respectively, was dependent on the presence of exogenous LPA (Fig. 3d and data not shown) and was stimulated by phosphorylation with cAMP-dependent protein kinase (Table 2). Purified recombinant endophilin I showed essentially the same specificity for LPA as substrate, as compared to other lysophospholipids, as did the enzyme purified from bovine brain (Table 2).

Given the original observation that the poly(L-proline) DMSO eluate obtained from brain cytosol, which was highly enriched in endophilin I (Fig. 1b), promoted SLMV formation in the perforated-cell system (Fig. 1a), it was important to verify that this eluate exhibited LPAAT activity. This was indeed the case (Fig. 3e).

Endophilin I binds fatty acyl-CoA and LPA

Endophilin I was depleted from brain cytosol upon passage over a palmitoyl-CoA agarose column, in contrast to the bulk of the cytosolic proteins and Grb2 (Fig. 4a), another SH3-domain-containing protein with an isoelectric point similar to that of endophilin I. Binding of endophilin I to palmitoyl-CoA agarose was prevented when cytosol was loaded onto the column in the presence of free palmitoyl-CoA (Fig. 4b). Likewise, endophilin I bound to palmitoyl-CoA agarose was eluted from the column by free palmitoyl-CoA (Fig. 4a). These results indicate that endophilin I binds fatty acyl-CoA.

To investigate the binding of endophilin I to LPA, we prepared a radioactive photoactivatable analogue of LPA, [^{32}P]1-(10-azi-stearoyl)-LPA. When a high-speed supernatant obtained from bacteria transformed with vector containing the insert encoding His_6-tagged endophilin I was subjected to UV-irradiation in the presence of the photoactivatable LPA, a ^{32}P-labelled 40K band was observed (Fig. 4c, left) that coincided with recombinant endophilin I detected by protein staining (Fig. 4c, right). Labelling of this band was dependent on UV-irradiation (Fig. 4c) and was blocked by excess unlabelled LPA (data not shown). The 40K band was not detected when a high-speed supernatant from bacteria transformed with vector lacking insert was used, in contrast to an endogenous bacterial 45K protein that was equally labelled in both supernatants (Fig. 4c). Similar photoaffinity labelling was observed for the GST–endophilin-I fusion protein (data not shown). We conclude that endophilin I binds LPA.

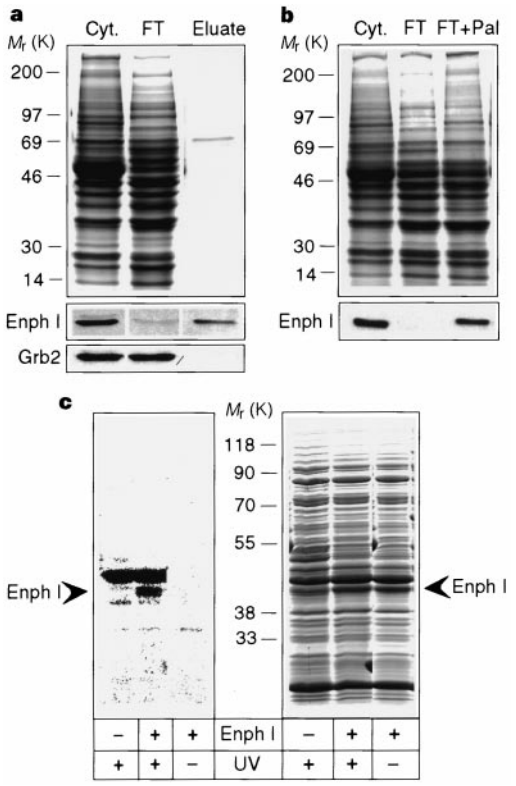

Figure 4 Endophilin I binds to fatty acyl-CoA and LPA. **a**, **b**, Binding of endophilin I from brain cytosol to palmitoyl-CoA agarose. Top panels: Coomassie-Blue-stained SDS-polyacrylamide gel of the cytosol loaded onto palmitoyl-CoA agarose (Cyt.), the corresponding flow-through obtained in the absence (**a**, **b**, FT) or presence (**b**, FT + Pal) of 40 mM free palmitoyl-CoA added to the cytosol before loading, and the eluate obtained upon addition of 4 mM free palmitoyl-CoA (**a**, Eluate). Bottom panels: Endophilin I (Enph I) and Grb2 immunoblots of the material shown in the top panels. In **a**, the eluate corresponds to 1/4 of the loaded cytosol and flow-through and, therefore, the exposure time of the endophilin I immunoblot for the eluate is four times that of the cytosol and flow-through. **c**, Photoaffinity labelling of recombinant endophilin I using [^{32}P]1-(10-azi-stearoyl)-LPA. The 280,000*g* supernatant obtained from a lysate (freezing/thawing) of bacteria transformed without (Enph I–) or with (Enph I+) the insert coding for His_6–endophilin I was incubated in the presence of [^{32}P]1-(10-azi-stearoyl)-LPA without (UV–) or with (UV+) UV irradiation, followed by SDS-PAGE, Coomassie-Blue staining (right panel) and phosphoimaging (left panel).

Effects of added LPA and fatty acyl-CoA

Addition of 1 μM LPA to the perforated-cell system did not significantly affect the basal SLMV formation observed with low-protein cytosol, but completely blocked the ability of exogenously added recombinant endophilin I to mediate SLMV formation (Fig. 5a). This is consistent with the interpretation that exogenously added LPA competitively prevents endophilin I from acting on LPA in the donor membrane.

To investigate the requirement for fatty acyl-CoA in SLMV formation mediated by endophilin I, we used the unsaturated

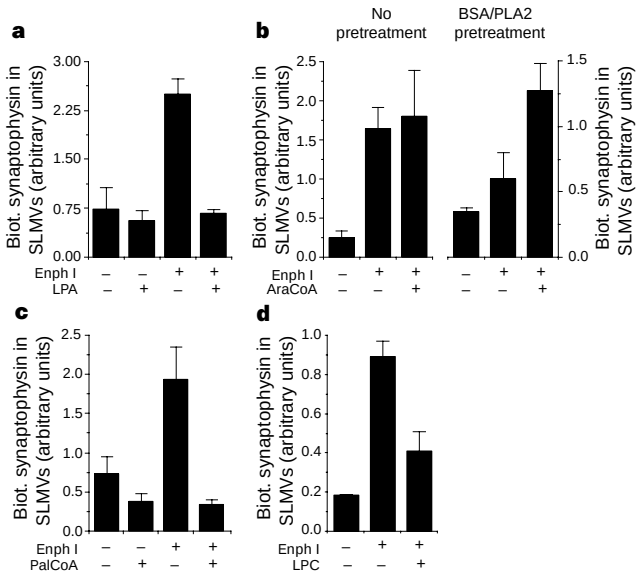

Figure 5 Effects of lysophospholipids and fatty acyl-CoA on endophilin-I-mediated SLMV formation. SLMV formation using perforated PC12 cells without (**a**, **b** left, **c**, **d**) or with (**b** right) BSA/PLA_2 pretreatment, supplemented with complete (and, for **b** and **c**, gel-filtered) brain cytosol at 0.75 mg protein per ml (**a**, **b** left, **c**, **d**) or 2.5 mg protein per ml (**b** right), in the absence (–) or presence (+) of the indicated additions: **a**, 1 μM LPA, 10 μg ml^{-1} purified (metal-chelate) recombinant His_6–endophilin I; **b**, 10 μM arachidonoyl-CoA (AraCoA), 10 μg ml^{-1} purified (metal-chelate and poly(L-proline)) recombinant His_6–endophilin I; **c**, 10 μM palmitoyl-CoA (PalCoA), 10 μg ml^{-1} purified (metal-chelate) recombinant His_6–endophilin I; **d**, 2 μM LPC, 10 μg ml^{-1} purified (poly(L-proline)) recombinant His_6–endophilin I. **a**–**d**, Data are the mean of three (**a**, **b** left, **c**, **d**) or two (**b** right) independent perforated-cell reactions; bars indicate s.d. or the variation of the individual values from the mean. Enph I, endophilin I.

fatty acid arachidonoyl-CoA rather than the saturated fatty acid palmitoyl-CoA because, upon stimulation of secretion, the increase in incorporation of arachidonate into phosphatidic acid is greater than that of palmitate[34]. In the standard perforated-cell system using gel-filtered low-protein cytosol, addition of 10 μM exogenous arachidonoyl-CoA in the presence of recombinant endophilin I did not increase SLMV formation above the level obtained by addition of endophilin I alone (Fig. 5b, left). Likewise, arachidonoyl-CoA did not increase the basal SLMV formation obtained without addition of endophilin I (data not shown). This indicated that, under these conditions, endogenous arachidonoyl-CoA was not rate-limiting. Presumably, in the presence of gel-filtered cytosol, the source of fatty acyl-CoA was fatty acid derived from membrane phospholipids through endogenous phospholipase A_2 (PLA_2) followed by activation by cytosolic fatty acyl-CoA synthase.

To remove free fatty acids and fatty acyl-CoA from the membranes, the perforated cells were pretreated with fatty acid-free bovine serum albumin (BSA). Including PLA_2 under non-lytic conditions (see Methods) during the BSA pretreatment reduced basal SLMV formation in the subsequent perforated-cell reaction to about half of that observed after BSA pretreatment in the absence of added PLA_2; addition of 10 μM arachidonoyl-CoA during the perforated-cell reaction following BSA/PLA_2 pretreatment restored basal SLMV formation to the original level (data not shown). We therefore used this pretreatment to show that arachidonoyl-CoA is required for endophilin-I-mediated SLMV formation. Compared to the marked stimulation of SLMV formation by endophilin I seen without BSA/PLA_2 pretreatment (Fig. 5b left), BSA/PLA_2 pretreatment greatly reduced endophilin-I-mediated SLMV formation in the absence of exogenously added arachidonoyl-CoA (Fig. 5b right); addition of 10 μM arachidonoyl-CoA doubled the endophilin-I-mediated SLMV formation (Fig. 5b right). We conclude that endophilin-I-mediated SLMV formation requires fatty acyl-CoA.

We next investigated whether palmitoyl-CoA, which, like arachidonoyl-CoA, can be used as substrate by endophilin I to generate phosphatidic acid (data not shown), also supported endophilin-I-mediated SLMV formation. In the standard perforated-cell system using low-protein cytosol, addition of 2.5 μM (data not shown) or 10 μM (Fig. 5c) of palmitoyl-CoA completely blocked endophilin-I-mediated SLMV formation, in contrast to arachidonoyl-CoA (Fig. 5b). Addition of 2 μM LPC, which was a much poorer substrate for endophilin I than LPA (Table 2), also inhibited endophilin-I-mediated SLMV formation (Fig. 5d).

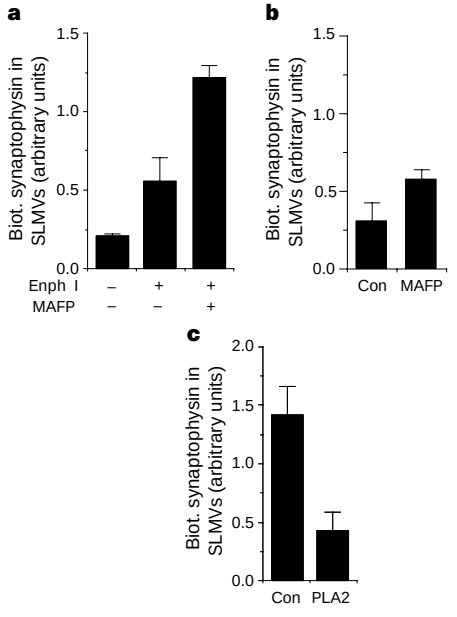

Figure 6 Effects of PLA_2 and the PLA_2 inhibitor MAFP on endophilin-I-mediated SLMV formation. SLMV formation in perforated PC12 cells using complete brain cytosol (0.75 mg protein per ml) in the absence (–, Con) and presence (+) of the indicated additions: **a**, 10 μg ml^{-1} purified (metal-chelate) recombinant His_6–endophilin I (Enph I), 10 μM MAFP; **b**, 10 μM MAFP; **c**, 10 μg ml^{-1} PLA_2 from *C. adamanteus*. Note that to quantify the reduction by PLA_2 below the control, the immunoblot was exposed longer than in the case of a stimulation above the control (such as **a**, **b**), resulting in higher than usual arbitrary units for the control value. **a**–**c**, Data are the mean of three independent perforated-cell reactions; bars indicate s.d.

A PLA_2 inhibitor potentiates SLMV formation

If SLMV formation mediated by endophilin 1 is due to the conversion of LPA to phosphatidic acid, one might expect that a PLA_2 inhibitor acts synergistically with endophilin I in SLMV formation because the reverse reaction, the hydrolysis of phosphatidic acid to LPA and free fatty acid, which presumably occurs during the perforated-cell reaction owing to the activity of cytosolic PLA_2, would be prevented. Indeed, the specific inhibitor of cytosolic calcium-dependent and -independent PLA_2, methyl arachidonyl fluorophosphonate (MAFP[38]), strongly potentiated endophilin-I-mediated SLMV formation (Fig. 6a). This observation indicates that endogenous cytosolic PLA_2 may be able to antagonize the action of endophilin I in SLMV formation.

In most of the experiments described above, the effects of recombinant endophilin I on SLMV formation were investigated in the presence of low-protein cytosol, which by itself supported a basal level of SLMV formation. Given the results of Fig. 1c, this basal SLMV formation can largely be attributed to the endophilin I endogenously present in low-protein cytosol (~6 μg ml^{-1}). Like the SLMV formation mediated by addition of exogenous endophilin I (Fig. 6a), the basal SLMV formation should therefore be sensitive to agents affecting hydrolysis of phosphatidic acid. Indeed, addition of MAFP moderately stimulated basal SLMV formation (Fig. 6b). Conversely, addition of exogenous PLA_2 derived from snake venom markedly reduced basal SLMV formation (Fig. 6c), the residual level being only slightly above that observed without addition of any cytosol (data not shown).

The role of the SH3 domain of endophilin I

Dynamin, which is an essential component of the machinery that mediates SLMV formation in our perforated-cell system[25], is recruited to, and forms rings at, the necks of synaptic vesicles budding from their donor membrane[4]. Endophilin I binds, by its SH3 domain, to the proline-rich region of dynamin[30]. We therefore investigated whether SLMV formation mediated by endophilin I involved protein–protein interaction through its SH3 domain. A ~34K deletion mutant of endophilin I lacking the SH3 domain (referred to as del-endophilin I) still exhibited LPAAT activity (Fig. 7a) but no longer mediated SLMV formation, at least not at the concentration tested (~10 μg ml^{-1}; Fig. 7b). This shows that protein–protein interaction of endophilin I through its SH3 domain is essential for its ability to mediate SLMV formation. Although endophilin I binds not only to dynamin[30] but also synaptojanin[30,31], we interpret the need for its SH3 domain in terms of an interaction with dynamin rather than synaptojanin because, in perforated PC12 cells supplemented with cytosol depleted of both dynamin and synaptojanin, addition of dynamin alone is sufficient to restore SLMV formation[25]. Specifically, we propose that the interaction with dynamin results in the recruitment of endophilin I, and hence its LPAAT activity, to the membrane of budding synaptic vesicles.

Discussion

We have provided several lines of evidence that endophilin I has LPAAT activity. First, endophilin I isolated from brain using ESPACE as the final purification step appears as a single 40K protein on analytical SDS- and 2D PAGE and exhibits LPAAT activity after

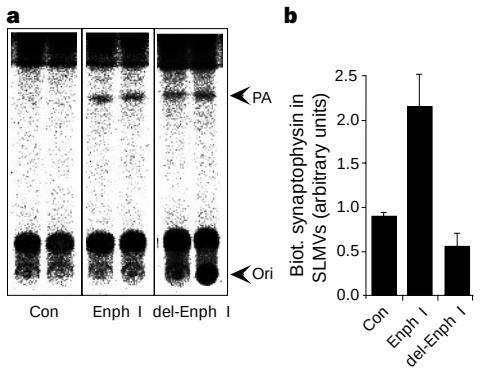

Figure 7 Endophilin I lacking its SH3 domain (del-endophilin I) still possesses LPAAT activity but does not promote SLMV biogenesis. **a**, Duplicate LPAAT assays using 5 μM [^{14}C]arachidonoyl-CoA and 10 μM LPA in the absence (Con) and presence of 10 μg ml^{-1} purified (metal-chelate) recombinant His$_6$–endophilin I (Enph I) and del-His$_6$–endophilin I (del-Enph I). PA, phosphatidic acid; Ori, origin. **b**, SLMV formation in perforated PC12 cells using complete brain cytosol (0.75 mg protein per ml) in the absence (Con) and presence of 10 μg ml^{-1} purified (metal-chelate) recombinant His$_6$–endophilin I and del-His$_6$–endophilin I. Data are the mean of three independent perforated-cell reactions; bars indicate s.d.

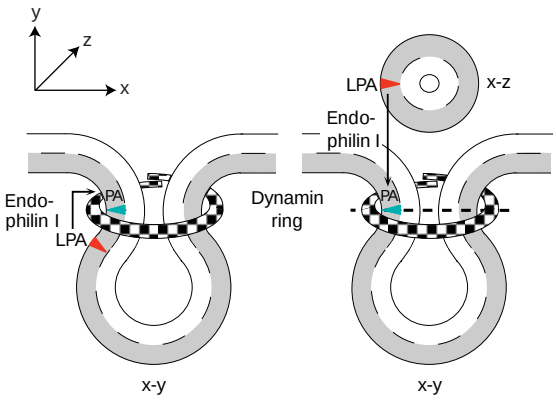

Figure 8 Role of endophilin-I-mediated conversion of LPA to phosphatidic acid (PA) in one of the steps of synaptic vesicle formation (fission). Left: nascent vesicle with neck surrounded by a dynamin ring (drawn in line with its snake[17] or Ferrari[49] function in endocytosis). The cytoplasmic leaflet of the lipid bilayer is shaded. Owing to its interaction with dynamin I (ref. 30), endophilin I is recruited to the neck of the nascent vesicle. The LPAAT activity of endophilin I (arrow) converts LPA by addition of arachidonate to PA, thereby changing an inverted-cone-shaped lipid inducing positive membrane curvature (red wedge) to a cone-shaped lipid inducing negative curvature (blue wedge) in the cytoplasmic leaflet. This may promote the transition from the bud (positive curvature) to the neck (negative curvature in the spatial x–y plane shown) that precedes fission. Right: in addition to the same view of the nascent vesicle as in the left panel, a cross-section at the neck (dashed line) is shown at the top. This illustrates the positive membrane curvature that exists in the cytoplasmic leaflet (shaded) at the neck in the spatial plane of the cross-section (x–z), in contrast to the negative curvature found upon 90° rotation of this spatial plane (x–y). The endophilin-I-catalysed conversion (arrow) of the positive-curvature-inducing lipid LPA (red wedge) to the negative-curvature-inducing lipid PA (blue wedge) may promote the constriction of the neck towards fission. Note that in addition to fission, other steps in vesicle formation (not illustrated) such as coated pit invagination are also associated with a positive-to-negative change in membrane curvature and that endophilin-I-mediated LPA-to-PA conversion may also operate in these steps.

renaturation. The protein clearly eluted with a higher apparent molecular mass than the transmembrane LPAATs described so far[39,40]; all of the latter migrate with apparent relative molecular masses of ~29–31K, and no such band was detected in the fractions containing the purified endophilin I and exhibiting LPAAT activity. Second, recombinant endophilin I exhibited LPAAT activity after various types of purification (GSH-column for GST–endophilin-I, metal-chelate column for His$_6$–endophilin-I, poly(L-proline) column for either fusion protein). Moreover, recombinant endophilin I was solely responsible for the LPAAT activity observed in the soluble fraction obtained from transformed bacteria lysed by freezing/thawing. Third, endophilin I binds to palmitoyl-CoA and was photoaffinity-labelled by a photoactivatable LPA analogue, showing that it physically interacts with its two substrates.

A phosphorylation-induced increase in LPAAT activity, apparently reflecting the stimulation of LPAAT activity in response to secretagogue originally observed in parotid acinar cells[34], has been observed in a postnuclear membrane fraction[36]. This led us to anticipate that this LPAAT activity would reside in a membrane-associated protein. We therefore used a crude membrane fraction as a source for LPAAT purification. How, then, can it be explained that this purification yielded endophilin I, which upon hypo-osmotic lysis of synaptosomes is largely recovered in the soluble fraction[31], consistent with it being a cytosolic protein? Presumably, the crude membrane fraction used as starting material for the solubilization of LPAAT, which was obtained from a relatively low-speed iso-osmotic supernatant, still contained synaptosomes (sealed nerve terminals) which, in line with the presynaptic localization of endophilin I (ref. 30), are enriched in this protein.

The observations that low-protein cytosol depleted of endophilin I barely supported SLMV formation in the perforated-cell system and that addition of recombinant endophilin I to this cytosol restored SLMV formation to the level obtained with high-protein cytosol indicate an essential role for endophilin I in this process. The function of endophilin I in SLMV formation appears to be mediated by its LPAAT activity. First, under conditions designed to lower the endogenous fatty acyl-CoA content of the perforated cells, endophilin-I-mediated SLMV formation was largely dependent on exogenous arachidonoyl-CoA. Second, exogenous LPA blocked endophilin-I-mediated SLMV formation, presumably by preventing the action of endophilin I on the endogenous LPA in the SLMV donor membrane. Third, endophilin-I-mediated SLMV formation was strongly promoted by the PLA$_2$ inhibitor MAFP, which would stabilize the effect of the LPAAT reaction catalysed by endophilin I, that is, an increase in the phosphatidic acid/LPA ratio.

There are several potential mechanisms by which the LPAAT activity of endophilin I could mediate SLMV formation. One is that the phosphatidic acid generated by endophilin I in the donor membrane either stimulates, by activating phosphatidylinositol-4-phosphate (PtdIns(4)P) 5-kinase[41], the formation of PtdIns(4,5)P$_2$, or increases phosphoinositide levels by serving as a precursor in their synthesis. A local increase in the PtdIns(4,5)P$_2$ level in the donor membrane may promote the recruitment of dynamin via its pleckstrin-homology domain, and thereby stimulate SLMV formation[8,41,42]. Phosphatidic acid may also directly promote dynamin-mediated changes in membrane shape, given that an increase in the amount of phosphatidic acid in liposomes favours the formation of dynamin-coated tubules[13]. However, we have observed that addition of phospholipase D (PLD), which increases phosphatidic acid by hydrolysing phosphatidylcholine, does not increase SLMV formation in the perforated-cell system although, in parallel experiments using another cell-free system, it did increase secretory vesicle formation from the trans-Golgi network (data not shown), confirming previous observations[43]. This may indicate that endophilin I mediates SLMV formation not simply because it increases phosphatidic acid, but also because it concomitantly consumes LPA.

This leads us to consider changes in membrane curvature as a central feature of the mechanism by which endophilin I mediates the formation of SLMVs and, by extrapolation, the recycling of synaptic vesicles. Synaptic vesicles are the smallest physiologically occurring vesicles of biological membranes known. The neck of a budding synaptic vesicle, especially when this budding occurs from the planar plasma membrane, is therefore characterized by greater membrane curvature than that of other membrane vesicles. Speci-

fically, the positive membrane curvature that exists in the cytoplasmic leaflet of a coated pit and bud changes to negative membrane curvature in one of the two spatial dimensions: at the edge of the coated pit as it invaginates from the planar plasma membrane to form a bud, and at the constricting neck of a bud proceeding to fission from either the planar plasma membrane or a tubular plasma membrane invagination. Inverted-cone-shaped membrane lipids and cone-shaped membrane lipids induce positive and negative membrane curvature, respectively[19,20]. LPA is thought to be an inverted-cone-shaped lipid, and phosphatidic acid (especially with arachidonate in position 2 of the glycerol backbone) a cone-shaped lipid[20]. Moreover, inverted-cone-shaped lipids and cone-shaped lipids have been proposed to affect membrane fusion in a differential manner[20,22]. It is therefore conceivable that endophilin I mediates synaptic vesicle formation because the conversion of LPA to an appropriate phosphatidic acid, catalysed by the LPAAT activity of endophilin I, induces the positive-to-negative membrane curvature change in the cytoplasmic leaflet that is required for coated pit invagination and, as shown in Fig. 8, the constriction of the neck of a budding synaptic vesicle during fission.

Such a mechanism would explain why the unsaturated fatty acid arachidonoyl-CoA supported endophilin-I-mediated SLMV formation, whereas the saturated fatty acid palmitoyl-CoA blocked this process. In line with its ability to use palmitoyl-CoA as substrate (data not shown), endophilin I may have generated a phosphatidic acid with palmitate in position 2. Such a phosphatidic acid may be non-productive for SLMV formation because its generation from LPA would result in a much less pronounced shape change of the lipid from inverted cone to cone than that upon addition of arachidonate.

Alternatively, palmitoyl-CoA, which, in contrast to arachidonoyl-CoA, is an inverted-cone-shaped lipid, may have blocked endophilin-I-mediated SLMV formation not as a substrate but by acting directly on the lipid bilayer, which would imply a profound sensitivity of SLMV formation to lipid shape. Direct evidence for an inhibition of endophilin-I-mediated SLMV formation by inverted-cone-shaped lipids was obtained using LPC (C10:0 in position 1). LPC is not a substrate for endophilin I and hence would presumably not interfere with endophilin-I-catalysed conversion of LPA to phosphatidic acid.

Previous models of dynamin function have suggested that this protein itself may operate as a 'pinchase' at the neck of synaptic and other endocytic vesicles[5,8]. However, evidence has been reported[16] that dynamin does not function as a force-generating GTPase but rather, like other members of the GTPase superfamily, activates a downstream effector. Our observations raise the possibility that endophilin I constitutes this effector, which would be recruited to the membrane, and perhaps activated, by dynamin to mediate fission. Consistent with this concept, the deletion mutant of endophilin I lacking the SH3 domain, which still exhibited LPAAT activity but presumably no longer bound to dynamin, did not mediate SLMV formation. Activation of endophilin I upon its dynamin-mediated recruitment to the membrane would also explain why the rate of acyl transfer of soluble endophilin I was relatively low ($\leq$17 mU mg^{-1} protein).

In mammals, endophilin I belongs to a protein family whose other members are endophilin II and endophilin III (originally called SH3p8 and SH3p13, respectively), which also interact with dynamin[30]. Like endophilin I, whose tissue distribution is indistinguishable from that of dynamin I, endophilins II and III co-distribute with dynamins II and III, respectively[30], consistent with the existence of endophilin I–dynamin I, endophilin II–dynamin II and endophilin III–dynamin III complexes. This raises the possibility that the mechanism of positive-to-negative membrane curvature change in vesicle formation that we propose (the conversion of an inverted-cone-shaped lipid to a cone-shaped lipid by addition of a fatty acyl chain to a lyso-glycero-lipid) operates not only in SLMV/synaptic vesicle formation mediated by endophilin I–dynamin I but, perhaps, also in the formation of other vesicles by endophilin II–dynamin II and endophilin III–dynamin III. Furthermore, this mechanism (operating not necessarily only with arachidonate) may not be confined to dynamin-dependent pinching-off of vesicles from donor membranes, but may be a common feature of vesicle formation and particularly membrane fission. Palmitoyl transfer to an unidentified acceptor is required in the pinching-off of Golgi-derived vesicles[44–46]. Perhaps this acceptor, too, is LPA, given the observation that BARS-50, a protein substrate of brefeldin A-dependent ADP-ribosylation, induces the fission of Golgi tubules by palmitoyl transfer to a membrane lipid (R. Weigert *et al.*, unpublished observation). □

Methods

SLMV formation

SLMV formation in perforated PC12 cells, using cell-surface-biotinylated synaptophysin as marker (abbreviated as 'Biot. synaptophysin' in the Figures) and the single 30% glycerol step centrifugation to isolate SLMVs, was carried out and quantified as described[25]. Differences in arbitrary units between Figure panels reflect differences in the exposure time of the synaptophysin immunoblots rather than in the efficiency of SLMV formation. In the standard control condition (cytosol containing 0.75 mg protein per ml), 0.8 $\pm$ 0.2% of the total biotinylated synaptophysin was recovered in SLMVs[25]. To address the role of fatty acyl-CoA we used gel-filtered cytosol (PD-10 column, Pharmacia; GGA buffer) supplemented with 1 mM GTP. LPA (L-α-lysophosphatidic acid, oleoyl (C18:1, (cis)-9), Sigma) was added from a 10 mM stock in LPA buffer (20 mM Hepes-KOH pH 7.4, 10 mM sucrose, 1 mM EDTA, 2.5 mg ml^{-1} fatty acid-free BSA (Boehringer)) sonicated (Sonorex super RK 102H) for 2 min; reactions without LPA contained the corresponding amount of LPA buffer. LPC (L-α-lysophosphatidylcholine, decanoyl (C10:0), Sigma), palmitoyl-CoA (Sigma) and arachidonoyl-CoA (Fluka) were added from 10 mM, 10 mM and 50 mM stocks in water, respectively. MAFP (Biomol Research Laboratories) was added from a 135 mM stock in DMSO; reactions without MAFP contained the corresponding amount of DMSO. PLA_2 from *Crotalus adamanteus* venom (CellSystems) was added from a 1 mg protein per ml stock in water. PLD from *Streptomyces chromofuscus* (Sigma) was added from a 100 U μl^{-1} stock in 10 mM Hepes-KOH pH 7.4 to a final concentration of 0.01–10 U ml^{-1}.

When investigating the role of arachidonoyl-CoA (Fig. 5b right), the pellet of perforated PC12 cells (~15 mg protein) was resuspended in 2 ml of the GGA/glutathione buffer[25] containing 10 mg ml^{-1} fatty-acid-free BSA, followed by addition of 50 μg ml^{-1} PLA_2 from *C. adamanteus* and incubation at 37 °C for 15 min. All subsequent steps were performed at 4 °C. The BSA/PLA_2-treated perforated cells were washed and resuspended in GGA/glutathione buffer and used for perforated-cell reactions.

Purification of LPAAT from bovine brain

All steps were carried out at 4 °C. Bovine brains were homogenized with 3 volumes (v/w) of buffer A (50 mM Tris-HCl, pH 7.4; 250 mM sucrose; 2 mM EDTA; 50 μM PMSF; 0.1% (v/v) 2-mercaptoethanol) in a Warring Blender-type homogenizer. A particulate fraction containing most of the LPAAT activity present in the homogenate was obtained by differential centrifugation as follows: the homogenate for 10 min at 1,000g_{av}, the supernatant for 30 min at 5,000g_{av}, the supernatant for 2 h at 60,000g_{max}. The pellet was resuspended in buffer A to 15 mg protein per ml and diluted five-fold with buffer B (25 mM Hepes-NaOH pH 7.4, 2 mM EDTA, 4 mM CHAPS, 0.1% (v/v) 2-mercaptoethanol). Insoluble material was removed by centrifugation for 1 h at 100,000g_{max}; the resulting supernatant, referred to as Extract (Table 1), was loaded onto a Q-Sepharose column and LPAAT-activity was eluted with a 0–1.5 M NaCl-gradient in buffer C (50 mM Tris-HCl, pH 7.4; 250 mM sucrose; 2 mM EDTA; 2 mM CHAPS, 0.1% (v/v) 2-mercaptoethanol). The fractions of peak II were combined, dialysed against buffer D (50 mM potassium phosphate, pH 6.2, 2 mM EDTA; 0.1% (v/v) Nonidet P-40; 0.1% (v/v) 2-mercaptoethanol), loaded onto an S-Sepharose column and LPAAT was eluted with a linear 0–0.75 M NaCl gradient in buffer D. LPAAT-containing fractions were combined, dialysed against buffer E (20 mM Tris-HCl, pH 7.4; 10% (w/v) glycerol; 2 mM EDTA; 0.1% (v/v) Nonidet P-40; 0.1% (v/v) 2-mercaptoethanol) and loaded onto a Mono Q HR 10/10 column, and LPAAT was eluted with a 0–1 M NaCl gradient in buffer E. LPAAT-containing fractions were combined, dialysed against buffer F (20 mM Tris-HCl, pH 7.4; 1 mM EDTA; 10% (w/v) glycerol; 100 mM NaCl; 0.1% (v/v) Nonidet P-40; 10 μM PMSF; 0.1% (v/v) 2-mercaptoethanol) and chromatographed on a Superdex 75 Hiload 16/60 column in buffer F. LPAAT-containing fractions were combined, concentrated using Centricon-30, loaded onto a Mono Q HR 5/10 anion-exchange column and LPAAT was eluted using a 0–1 M NaCl gradient in buffer E. LPAAT-containing fractions were concentrated using Centricon-30, diluted with one volume of 2× Laemmli sample buffer, heated for 2 min to 95 °C, loaded (300 μl) onto the cylindrical SDS-polyacrylamide gel column of a Model 491 Prep Cell (Biorad) electrophoresis apparatus and subjected to ESPACE according to the recommendations of the manufacturer. Fractions of 2 ml were collected and concentrated to ~0.1 ml using Centricon-30, and aliquots were analysed by analytical SDS-PAGE (Fig. 2a). Fractions containing the purified protein of ~40K were diluted with buffer E (2 ml buffer E per 0.1 ml fraction) and concentrated to 0.1 ml by Centricon-30 centrifugation. This was repeated twice and, after this renaturation protocol, aliquots of the fractions were assayed for LPAAT activity (Fig. 2b). Fractions containing the ~40K protein as the only detectable band and possessing LPAAT activity were combined and used for 2D-PAGE, sequence analysis and determination of substrate specificity.

Poly(L-proline) Sepharose adsorption and elution

All steps were performed at 4 °C. Rat brain cytosol[25] (1.5–3 ml, 7.5 mg protein per ml) was subjected to a single passage over a column containing ~1 ml of packed poly(L-proline)-coated Sepharose beads[28] and the flow-through was collected (depleted cytosol). The column was washed with 20 ml of GGA buffer[25] and eluted either directly with 2 ml of 8 M urea containing 10 mM Hepes-KOH, pH 7.4 or with 2 ml of 30% (w/v) DMSO diluted in GGA buffer followed by 2 ml of 8 M urea containing 10 mM Hepes-KOH, pH 7.4. The DMSO eluate (and, as control, 30% DMSO in GGA buffer) was extensively dialysed against GGA buffer containing 5 mM reduced glutathione, followed by concentration using Centricon-10 to ~200 μl, which contained ~30 μg of endophilin I as judged by SDS-PAGE using recombinant endophilin I as standard.

Protein identification

For MALDI, protein bands were excised from the gel and in-gel digested with trypsin as described[47]. Peptide-mass mapping was performed on a Bruker Reflex mass spectrometer, and the list of peptide masses searched against a non-redundant protein sequence database with an accuracy better than 50 p.p.m.

For protein sequencing of tryptic peptides, ~10 μg of the 40K protein purified from bovine brain through the ESPACE step was digested twice for 2 h at 37 °C with 0.1 μg TPCK-trypsin. Peptides were separated by RP-HPLC (VYDAC 218 TP) using a 0.1% TFA/acetonitrile gradient and sequenced by the Edman method using an ABI sequenator.

Palmitoyl-CoA agarose adsorption and elution

All steps were performed at 4 °C. Rat brain cytosol (0.8 ml, 7.5 mg protein per ml) was subjected, with or without 40 mM added free palmitoyl-CoA, to a single passage over a column containing 1.5 ml of packed palmitoyl-CoA agarose beads (Sigma, equilibrated in GGA buffer), and the flow-through was collected. The column was washed with 20 ml of GGA buffer and eluted with 0.5 ml of GGA buffer containing 4 mM free palmitoyl-CoA (kept in the column overnight) followed by 3.5 ml of GGA buffer (total eluate 3.5 ml).

Recombinant endophilin I

A full-length endophilin I cDNA was generated byPCR (Pwo) using a mouse brain cDNA library and primers (sense primer 5′-CGAATACGAGGATCCATGTCGGTGG-CAGGGCTGAAG, antisense primer 5′-GCTTAACGAGAATTCCTAATGGGGCAGAG-CAACCAG) designed according to the sequence of mouse endophilin I (ref. 18). The cDNA was cloned into pGEX2T (Pharmacia) and pQE30 (Qiagen) to obtain GST- and His_6-tagged fusion proteins, respectively.

A cDNA coding for a truncated endophilin I (amino acids 1–293, referred to as del-endophilin I), which lacks the SH3 domain, was generated by PCR using the full-length endophilin I cDNA, the above sense primer and the antisense primer 5′-TCGCGAAGCGGTACCGATCTGATCCATTTGGACACCTGG, which encodes a stop codon after amino acid 293 and contains a *Kpn*I restriction site. The PCR product was digested with *Bam*H1 and *Kpn*I and ligated into pQE30 to obtain His_6–del-endophilin I.

The fusion proteins were expressed in BL21 or BL21-d (inducible for lysozyme) bacteria (Stratagene). Bacteria were lysed by two cycles of rapid freezing/thawing in PBS (25 ml per 1-L culture pellet). All subsequent steps were performed at 4 °C. After addition of aprotinin (5 μg ml^{-1}), leupeptin (10 μg ml^{-1}), benzamidine (1 mM), PMSF (0.5 mM) and DNaseI (10 μg ml^{-1}, grade I, Boehringer) and incubation for 15 min, the lysate was centrifuged for 10 min at 10,000*g* and the resulting supernatant for 75 min at 280,000*g*. The high-speed supernatant (~6 mg protein per ml) was used for LPAAT assays (Fig. 3a), LPA-photoaffinity labelling (Fig. 4c), and the purification of recombinant endophilin I by either poly(L-proline) affinity chromatography (used to obtain the data shown in Figs 1c, 3b, c and 5b) or metal-chelate chromatography (used to obtain data not shown). In some experiments, pelleted bacteria were lysed (all steps at 4 °C) in 50 mM sodium phosphate pH 8.0, 300 mM NaCl, 10 mM imidazol, 2 mM Pefabloc (Boehringer) using sonication followed by addition of Triton X-100 (1% (v/v) final) and centrifugation for 15 min at 12,000g_{max}; the resulting supernatant was used for the purification of recombinant endophilin I using either metal-chelate chromatography (used to obtain the data shown in Figs 3d, 5, 6a, b, 7 and Table 2) or GSH affinity chromatography (used to obtain the data shown in Table 2).

Recombinant endophilin I was purified by poly(L-proline)-affinity chromatography as described above, except that DMSO was removed from the eluate by gel filtration using a PD-10 column equilibrated in GGA buffer followed by concentration using Centricon-10. Purification of recombinant endophilin I by metal-chelate chromatography was performed using Talon (Clontech) equilibrated with 50 mM NaH_2PO_4 pH 8.0, 300 mM NaCl, 10 mM imidazol, 2 mM Pefabloc; washing and elution used the same buffer except that imidazol was increased to 20 mM and 150 mM, respectively. Affinity chromatography using GSH-agarose was performed according to standard procedures. There was no obvious difference with regard to LPAAT activity and SLMV formation between the recombinant His_6–endophilin I purified by poly(L-proline) affinity chromatography from bacteria lysed by freezing/thawing, that purified by metal-chelate chromatography from such bacterial lysate, and that purified by metal-chelate chromatography from bacteria lysed by sonication/Triton X-100 (data not shown). As control, induced bacteria transformed with vector lacking the endophilin I insert were subjected in parallel to the same procedures of lysis, centrifugation and affinity chromatography, as indicated in the Figure legends.

Photoaffinity labelling using [^{32}P]1-(10-azi-stearoyl)-LPA

10-azi-stearic acid was prepared from 10-keto-stearic acid methyl ester (methyl 10-oxooctadecanoate, Aldrich). AtT-20 cells (one 10-cm dish) were grown for 16 h in 8 ml of phosphate-free DMEM (Sigma) supplemented with 18% serum (horse serum/FCS 2/1, delipidated by extraction with organic solvent (C.T., Y. Wang & W.B.H., manuscript in preparation)) and containing ~70 μM 10-azi-stearic acid (solubilized in serum[48]) and 1.5 mCi carrier-free inorganic [^{32}P]phosphate. The cells were extracted with chloroform/methanol and the chloroform phase subjected to thin-layer chromatography (TLC) using silica gel 60 (0.25 mm, Merck) and chloroform/methanol/water 65/35/8 as solvent. Phosphatidylcholine (PC, identified by minimal iodine vapour) was scraped from the plate, extracted using chloroform/methanol/water 65/35/8 and dried. After redissolving in 800 μl of diethylether/methanol 98/2, PC was converted to LPC using 250 μg PLA_2 (*C. adamanteus*) for 2 h at 25 °C (ref. 50). The whole reaction mixture was dried, redissolved in 500 μl 20 mM Tris-HCl pH 7.6, 5 mM $CaCl_2$, 1% Triton X-100, and after addition of PLD (1000 U, *S. chromofuscus*, Sigma) vigorously shaken at 30 °C for 2 h to convert LPC to LPA. After drying, lipids were dissolved in 300 μl chloroform/methanol/water 65/35/8 and subjected to TLC (chloroform/methanol/water/AcOH 65/35/8/6). The region of the thin-layer plate containing the [^{32}P]1-(10-azi-stearoyl)-LPA (identified by phosphoimaging and deduced from the mobility of LPA) was scraped and extracted with chloroform/methanol/water/AcOH 65/35/8/6. The yield of the final product was ~8 μCi.

For each photoaffinity-labelling reaction, 20 μl of [^{32}P]1-(10-azi-stearoyl)-LPA (10 μCi ml^{-1}, specific activity in the range of 0.1–1 μCi $μg^{-1}$) was dried and redissolved in 25 μl of 50 mM Hepes-NaOH pH 8.0 under sonication for 2 min. After addition of 50 μl of GGA buffer and 25 μl of 280,000*g* supernatant (150 μg protein) from a lysate of bacteria transformed without or with the insert coding for His_6–endophilin I, the samples were either placed under the filtered, focused beam (>310 nm) of a mercury lamp and UV-irradiated for 1 min at room temperature or kept for 1 min at room temperature without UV irradiation, followed in either case by addition of Laemmli sample buffer.

LPAAT assays

For the results shown in Fig. 2b and Tables 1 and 2, LPAAT activity was assayed in a final reaction volume of 200 μl containing, in addition to appropriate aliquots of the fractions obtained during and after purification, 10 mM Tris-HCl, pH 7.4; 0.1 mM EDTA, 25 mM sucrose; 0.05% (w/v) BSA; 100 μM of LPA (1-oleoyl) (or the other lyso-phospholipids indicated in Table 2); 40 μM [^{14}C]oleoyl-CoA (10–15 μCi mol^{-1}). To determine the substrate specificity of purified and recombinant endophilin I, 7 μg, 2 μg and 10 μg of endophilin I purified from bovine brain, His_6–endophilin I, and GST–endophilin I, respectively, was used per assay. Reactions were carried out for 10 min at 37 °C and terminated by the addition of 2 ml chloroform/methanol (2/1), followed by addition of 1 ml 0.1 M KCl. The organic phase was collected, dried, and subjected to TLC using chloroform/acetone/methanol/acetic acid/water (50/20/10/10/5). Radioactivity in phosphatidic acid on the TLC plates was determined using a Berthold thin-layer radioactivity scanner.

For determining the effect of phosphorylation of endophilin I on its LPAAT activity, we incubated 2.2 μg of either endophilin I purified from bovine brain, His_6–endophilin I or GST–endophilin I for 30 min at 37 °C in a final reaction volume of 20 μl containing in addition 40 mM Hepes–NaOH pH 7.4, 9 mM $MgCl_2$, 0.23 mM ATP and 7.5 μg ml^{-1} catalytic subunit of PKA. After the phosphorylation reaction, samples were subjected to LPAAT assay as above. The LPAAT activity observed after a phosphorylation reaction in the absence of added PKA was similar to that observed without performing the phosphorylation reaction.

For the results shown in Figs 3 and 7, aliquots of 1-[^{14}C]arachidonoyl-CoA (75-750 nCi, 56 mCi per mmol, Moravek Biochemicals) in ethanol:water (1:1) were dried in a SpeedVac and each dissolved in 150 μl of GGA buffer containing 5 mM reduced glutathione followed by sonication for 2 min. The tubes were then transferred to ice and brought to a final reaction volume of 300 μl by sequential additions as follows: (1) 137 μl or 122 μl of GGA buffer depending on the source of endophilin I to be added; (2) 3 μl of either the 10 mM LPA stock (see above), 1 mM LPA (made by 10-fold dilution of the 10 mM stock with LPA buffer followed by sonication for 4 min) or LPA buffer; (3) 10 μl of GGA buffer without or with ~3 μg of recombinant endophilin I, or 25 μl of the dialysed, concentrated and glycerol-diluted DMSO eluate without or with ~1.5 μg of endophilin I. Reactions were carried out for 15 min at 37 °C and terminated by addition of 300 μl ice-cold 0.8 M KCl, 0.2 M H_3PO_4. Samples were mixed with 900 μl chloroform/methanol (2:1) and centrifuged for 5 min at 10,000*g*. The lower phase was collected, dried, redissolved in 35 μl of chloroform/methanol/water (2:1:0:1), subjected (along with a ^{14}C-phosphatidic acid standard, NEN) to TLC using silica gel 60 and chloroform/pyridine/formic acid (50:30:7) as solvent, and analysed by phosphoimaging.

Miscellaneous

Recombinant human profilin I and mouse profilin II were obtained as described[27]. Two-dimensional PAGE was performed using ampholytes pH 3-10 for isoelectric focusing. A rabbit antiserum specifically recognizing endophilin I was obtained from Eurogentec, using the synthetic peptide (AcNH-KPRMSLEFATGDGT-$CONH_2$), corresponding to residues 258–271 of rat endophilin I (ref. 30), coupled to KLH-Glu as antigen. Anti-Grb2 antibody was obtained from Transduction Laboratories.

Received 9 June; accepted 26 July 1999.

1. Matsuoka, K. *et al.* COPII-coated vesicle formation reconstituted with purified coat proteins and chemically defined liposomes. *Cell* **93,** 263–275 (1998).
2. Spang, A., Matsuoka, K., Hamamoto, S., Schekman, R. & Orci, L. Coatomer, ARF1p, and nucleotide are required to bud coat protein complex I-coated vesicles from large synthetic liposomes. *Proc. Natl Acad. Sci. USA* **95,** 11199–11204 (1998).
3. Bremser, M. *et al.* Coupling of coat assembly and vesicle budding to packaging of putative cargo receptors. *Cell* **96,** 495–506 (1999).
4. Takei, K., McPherson, P. S., Schmid, S. L. & De Camilli, P. Tubular membrane invaginations coated by

dynamin rings are induced by GTP-γS in nerve terminals. *Nature* **374,** 186–190 (1995).
5. Warnock, D. E. & Schmid, S. L. Dynamin GTPase, a force-generating molecular switch. *BioEssays* **18,** 885–893 (1996).
6. Cremona, O. & De Camilli, P. Synaptic vesicle endocytosis. *Curr. Opin Neurobiol.* **7,** 323–330 (1997).
7. Schmid, S. Clathrin-coated vesicle formation and protein sorting: an integrated process. *Annu. Rev. Biochem.* **66,** 511–548 (1997).
8. Schmid, S. L., McNiven, M. A. & De Camilli, P. Dynamin and its partners: a progress report. *Curr. Opin. Cell Biol.* **10,** 504–512 (1998).
9. Hirst, J. & Robinson, M. S. Clathrin and adaptors. *Biochim. Biophys. Acta* **1404,** 173–193 (1998).
10. Vallee, R. B. & Okamoto, P. M. The regulation of endocytosis: identifying dynamin's binding partners. *Trends Cell Biol.* **5,** 43–47 (1995).
11. Hinshaw, J E. & Schmid, S. L. Dynamin self-assembles into rings suggesting a mechanism for coated vesicle budding. *Nature* **374,** 190–192 (1995).
12. Sweitzer, S. M. & Hinshaw, J. E. Dynamin undergoes a GTP-dependent conformational change causing vesiculation. *Cell* **93,** 1021–1029 (1998).
13. Takei, K. *et al.* Generation of coated intermediates of clathrin-mediated endocytosis on protein-free liposomes. *Cell* **94,** 131–141 (1998).
14. Stowell, M. H. B., Marks, B., Wigge, P. & McMahon, H. T. Nucleotide-dependent conformational changes in dynamin: evidence for a mechanochemical molecular spring. *Nature Cell Biol.* **1,** 27–32 (1999).
15. Roos, J. & Kelly, R. B. Is dynamin really a 'pinchase'? *Trends Cell Biol.* **7,** 257–259 (1997).
16. Sever, S., Muhlberg, A. B. & Schmid, S. L. Impairment of dynamin's GAP domain stimulates receptor-mediated endocytosis. *Nature* **398,** 481–486 (1999).
17. Kirchhausen, T. Boa constrictor or rattlesnake? *Nature* **398,** 470–471 (1999).
18. Sparks, A. B., Hoffmann, N. G., McConnell, S. J., Fowlkes, D. M. & Kay, B. K. Cloning of ligand targets: systematic isolation of SH3 domain-containing proteins. *Nature Biotechnol.* **14,** 741–744 (1996).
19. Lipowsky, R. Domain-induced budding of fluid membranes. *Biophys. J.* **64,** 1133–1138 (1993).
20. Chernomordik, L., Kozlov, M. M. & Zimmerberg, J. Lipids in biological membrane fusion. *J. Membrane Biol.* **146,** 1–14 (1995).
21. Düzgünes, N. in *Trafficking of Intracellular Membranes* (eds Pedroso de Lima, M. C., Düzgünes, N. & Hoekstra, D.) 97–129 (Springer, Heidelberg, 1995).
22. Chernomordik, L. V., Leikina, E., Frolov, V. Bronk, P. & Zimmerberg, J. An early stage of membrane fusion mediated by the low pH conformation of influenza hemagglutinin depends upon membrane lipids. *J. Cell Biol.* **136,** 81–93 (1997).
23. White, J. M. Membrane fusion. *Science* **258,** 917–924 (1992).
24. Kozlov, M. M. & Chernomordik, L. V. A mechanism of protein-mediated fusion: coupling between refolding of the Influenza hemagglutinin and lipid rearrangements. *Biophys. J.* **75,** 1384–1396 (1998).
25. Schmidt, A. & Huttner, W. B. Biogenesis of synaptic-like microvesicles in perforated PC12 cells. *Methods: A Companion to Methods Enzymol.* **16,** 160–169 (1998).
26. Schmidt, A., Hannah, M. J. & Huttner, W. B. Synaptic-like microvesicles of neuroendocrine cells originate from a novel compartment that is continuous with the plasma membrane and devoid of transferrin receptor. *J. Cell Biol.* **137,** 445–458 (1997).
27. Witke, W. *et al.* In mouse brain profilin I and II associate with regulators of the endocytic pathway and actin assembly. *EMBO J.* **17,** 967–976 (1998).
28. Janmey, P. A. Polyproline affinity method for purification of platelet profilin and modification with pyrene-maleimide. *Methods Enzymol.* **196,** 92–99 (1991).
29. Micheva, K. D., Ramjaun, A. R., Kay, B. K. & McPherson, P. S. SH3 domain-dependent interactions of endophilin with amphiphysin. *FEBS Lett.* **414,** 308–312 (1997).
30. Ringstad, N., Nemoto, Y. & De Camilli, P. The SH3p4/SH3p8/SH3p13 protein family: binding partners for synaptojanin and dynamin via a Grb2-like Src homology 3 domain. *Proc. Natl Acad. Sci. USA* **94,** 8569–8574 (1997).
31. De Heuvel, E. *et al.* Identification of the major synaptojanin-binding proteins in brain. *J. Biol. Chem.* **272,** 8710–8716 (1997).
32. Shupliakov, O. *et al.* Synaptic vesicle endocytosis impaired by disruption of dynamin–SH3 domain interactions. *Science* **276,** 259–263 (1997).
33. Desnos, C. Clift-O'Grady, L. & Kelly, R. B. Biogenesis of synaptic vesicles *in vitro*. *J. Cell Biol.* **130,** 1041–1049 (1995).
34. Söling, H.-D., Machado-De Domenech, E., Kleineke, J. & Fest, W. Early effects of β-adrenergic and muscarinic secretagogues on lipid and phospholipid metabolism in guinea pig parotid acinar cells. *J. Biol. Chem.* **262,** 16786–16792 (1987).
35. Söling, H.-D. *et al.* Mechanisms of short-term (second range) regulation of the activities of enzymes of lipid and phospholipid metabolism in secretory cells. *Adv. Enzyme Regul.* **28,** 35–50 (1989).
36. Söling, H.-D., Fest, W., Schmidt, T., Esselmann, H. & Bachmann, V. Signal transmission in exocrine cells is associated with rapid activity changes of acyltransferases and diacylglycerol kinase due to reversible protein phosphorylation. *J. Biol. Chem.* **264,** 10643–10648 (1989).
37. Coleman, J. Characterization of the *Escherichia coli* gene for 1-acyl-sn-glycerol-3-phosphate acyl-transferase (plsC). *Mol. Gen. Genet.* **232,** 295–303 (1992).
38. Lio, Y. C., Reynolds, L. J., Balsinde, J. & Dennis, E. A. Irreversible inhibition of Ca^{2+}-independent phospholipase A2 by methyl arachidonyl fluorophosphonate. *Biochim. Biophys. Acta* **1302,** 55–60 (1996).
39. Eberhardt, C., Gray, P. W. & Tjoelker, L. W. Human lysophosphatidic acid acyltransferase: cDNA cloning, expression, and localization to chromosome 9q34.3. *J. Biol. Chem.* **272,** 20299–20305 (1997).
40. West, J. *et al.* Cloning and expression of two lysophosphatidic acid acyltransferase cDNAs that enhance cytokine-induced signaling responses in cells. *DNA Cell Biol.* **6,** 691–701 (1997).
41. De Camilli, P., Emr, S. D., McPherson, P. S. & Novick, P. Phosphoinositides as regulators in membrane traffic. *Science* **271,** 1533–1538 (1996).
42. Warnock, D. E. & Schmid, S. L. Dynamin GTPase, a force-generating molecular switch. *BioEssays* **18,** 885–893 (1996).
43. Tüscher, O., Lorra, C., Bouma, B., Wirtz, K. W. A. & Huttner, W. B. Cooperativity of phosphatidy-linositol transfer protein and phospholipase D in secretory vesicle formation from the TGN—phosphoinositides as a common denominator? *FEBS Lett.* **419,** 271–275 (1997).
44. Glick, B. S. & Rothman, J. E. Possible role for fatty acyl-coenzyme A in intracellular protein transport. *Nature* **326,** 309–312 (1987).
45. Pfanner, N. *et al.* Fatty acyl-coenzyme A is required for budding of transport vesicles from Golgi cisternae. *Cell* **59,** 95–102 (1989).
46. Ostermann, J. *et al.* Stepwise assembly of functionally active transport vesicles. *Cell* **75,** 1015–1025 (1993).
47. Shevchenko, A. *et al.* Linking genome and proteome by mass spectrometry: large-scale identification of yeast proteins from two dimensional gels. *Proc. Natl Acad. Sci. USA* **93,** 14440–14445 (1996).
48. Spector, A. A. & Hoak, J. C. An improved method for the addition of long-chain free fatty acid to protein solutions. *Anal. Biochem.* **32,** 297–302 (1969).
49. Morris, S. A. & Schmid, S. L. The Ferrari of endocytosis? *Curr. Biol.* **5,** 113–115 (1995).
50. Kates, M. *Techniques in Lipidology* (Elsevier, Amsterdam, 1986).

Acknowledgements

We thank L. Chernomordik, D. Corbeil, M. J. Hannah and I. Trompeter for advice and discussion; M. Fischer and D. Hesse for technical assistance; and A. Summerfield for artwork. M.W. was supported by predoctoral fellowships from the Friedrich-Ebert-Stiftung and the Graduiertenkolleg 'Molekularbiologische Analyse pathophysiologischer Prozesse'. W.B.H. and H.-D.S. were supported by grants from the Fonds der Chemischen Industrie and the Deutsche Forschungsgemeinschaft.

Correspondence and requests for materials should be addressed to W.B.H. (e-mail: whuttner@sun0.urz.uni-heidelberg.de) or H.-D.S. (hsoelin@gwdg.de).